

# Application of Digital Phase-shift Shadow Moiré to Micro Deformation Measurements of Curved Surfaces

J. Degrieck, W. Van Paepegem\* and P. Boone

Ghent University, Dept. of Mechanical Construction and Production,  
Sint-Pietersnieuwstraat 41, 9000 Gent, Belgium

## Abstract

The shortcomings of conventional shadow Moiré topography have in the past been improved by means of the phase-shift method which enhances the sensitivity and allows to process the fringe patterns automatically. This paper presents a digital implementation of the phase-shifting process which requires only one image to be taken. The grating lines, projected onto the deformed object surface, are captured directly with a digital camera. Next the reference grating is superimposed numerically onto the projected grating lines. Then a number of phase-shifts are performed taking into account the non-linearities in the expression for the height-dependent intensity field. Experimental results prove that these non-linearities can considerably affect the micro deformation measurements of curved surfaces. The proposed method is very efficient and eliminates all causes of erroneous measurements due to miscalibration of phase-stepping devices.

**Keywords:** shadow Moiré, topography, digital phase-shift.

## 1. Introduction

Moiré techniques are straightforward methods for contactless non-destructive metrological measurements. Moiré topography in particular is a widely used means for shape contouring of three-dimensional objects. In general Moiré topography can be classified into two main categories: projection Moiré and shadow Moiré, according to the optical arrangement used.

In the case of a standard projection Moiré system, a precisely matching pair of gratings is typically used. The projection grating is placed in front of the light source and the reference grating or camera grating is placed in front of the camera. The projected beam of light is amplitude-modulated with the pitch of the grating. When this beam falls on the object surface, the phase of the spatial carrier is modulated by the shape of the object surface.

When using phase-shift projection Moiré [1], the camera grating is phase-shifted against the projection grating. This technique can be applied for precision measurement of fine objects.

In a digital projection Moiré system, the reference grating is omitted and the deformed projected grating is imaged directly by the camera. This captured grating is then demodulated numerically. Two images are required: the fringe projection on the reference plane and the object surface, respectively [2]. When applying the spatially parallel phase-shift technique, only one interferogram is required for the whole fringe pattern analysis [3].

The second category is the shadow Moiré technique. A grating is positioned close to the object and its shadow is observed through the grating. The grating lines and the shadow lines interfere, producing fringes which represent surface contours of equal height and describe the shape of the surface. A great deal of supplementary information in the gray level variation can

---

\* Corresponding author (Fax: +32-(0)9-264.35.87, E-mail: Wim.VanPaepegem@rug.ac.be).

be revealed by using the phase-shift method. The phase-shift is obtained by changing the object-to-grating distance [4,5]. When adopting the concept of digital speckle pattern interferometry (DSPI) phase-shifting methods, the grating can be placed in the illumination path only, and the resulting Moiré fringes are created by a subtraction like in normal DSPI operations. The phase of the fringes is shifted by a translation of the grating in its own plane [6].

This paper presents a digital phase-shift shadow Moiré technique, where only one image is captured: the projected grating lines onto the deformed object surface. The reference grating is superimposed numerically and a digital phase-shift method is performed. Although the height-dependent non-linearities are often neglected, it is shown here that these non-linearities are very important when measuring small deformations of curved surfaces. Finally, due to the simple optical arrangement, the errors caused by optical settings are eliminated and this makes the procedure very suitable for measurements of dynamic phenomena.

## 2. Review of the standard phase-shift shadow Moiré method

First the theory for standard shadow Moiré topography, as developed by Meadows et al. [7] and Takasaki [8,9], is shortly reviewed.

In Figure 1, the shadow Moiré setup is shown. The light source and the observer are assumed to be pointlike and are placed at a finite distance from the grating.

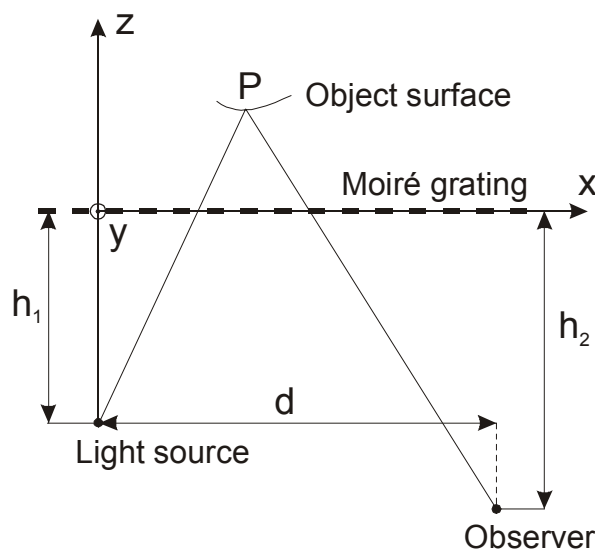


**Figure 1** Moiré contouring system with the light source and the observer at finite distances from the grating.

The intensity modulation of the grid is given by:

$$T(x) = \frac{1}{2} + \frac{1}{2} \sin\left(\frac{2\pi x}{p}\right) \quad (1)$$

where  $p$  is the period of the grid. Seen through a real lens system, a square wave grating can also be approximated by a sine wave grating. It has then been calculated by Meadows et al. [7] that, if the observer views the object surface through a small aperture (theoretically

assumed to be pointlike), the intensity distribution at a point (x,y,z) on the surface as seen by the observer, is given by Equation (2):

$$I_3(x, y) = \underbrace{\frac{I}{r^2} \cos(\phi(x, y, z(x, y))) \left[ \frac{1}{2} + \frac{1}{2} \sin \frac{2\pi h_1 x}{p(h_1 + z)} \right]}_{\text{term 1}} \times \underbrace{\left[ \frac{1}{2} + \frac{1}{2} \sin \frac{2\pi}{p} \left( \frac{dz + h_2 x}{h_2 + z} \right) \right]}_{\text{term 2}} \quad (2)$$

where  $I$  is the intensity of the light source,  $r$  is the distance from the light source to a particular portion of the surface being illuminated and  $\phi$  is the angle between the incident ray and the normal to the surface. The first term at the right side of the equation is the intensity of the shadow of the grid projected by the pointlike light source onto the surface, while the second term comprises the influence of the intensity transmission function of the sinusoidal grid,  $p$  being the period of the grid.

If and only if the light source and the observer are placed at the same distance from the grating (i.e.  $h_1 = h_2$ ), a term is produced in the expression for  $I_3(x,y)$  which is solely dependent on  $z$ . The contour information is then revealed by the term [7]:

$$(C/2) \cos \left[ \frac{2\pi dz}{p(h+z)} \right] \quad (3)$$

where  $C$  is a constant, defined in [7].

However the difference in height between two points cannot be determined simply by counting the number of fringes between them, because the fringes in Equation (3) do not vary sinusoidally with  $z$ . Therefore Equation (3) is often simplified by assuming that  $z \ll h$  and then the spatial frequency is given by  $d/(p \cdot h)$ .

Because fringe patterns must be analysed by tracing the centre-lines of the fringes and counting the height values, the phase-shift method has been introduced in shadow Moiré topography. The main advantages are that fringe pattern analysis can be done automatically and that the revealed information in the gray level variation solves the sign ambiguity. Moreover a much better resolution is acquired by using the additional information in the gray level.

The standard procedure for the phase-shift shadow Moiré method is based on the following equations [10]:

$$I_k(x, y) = A(x, y) + B(x, y) \cdot \cos \left( \frac{2\pi d(z + \delta_k)}{ph} \right) \quad \delta_k = \frac{k-1}{m} \cdot \frac{ph}{d} \quad (4)$$

where  $I_k(x,y)$  is the recorded fringe pattern for the  $k$ -th shift ( $k = 1, \dots, m$ ),  $d$  is the distance between the light source and the observer,  $h$  ( $h = h_1 = h_2$ ) is the distance from the grating to the light source and the observer,  $p$  is the pitch of the Moiré grating and  $A(x,y)$  and  $B(x,y)$  are respectively the background and local contrast. Here it is again assumed that  $z \ll h$ .

The system of equations (4) is often formulated as:

$$I_k(x, y) = A(x, y) + B(x, y) \cdot \cos[\Delta\phi(x, y) + \phi_k] \quad k = 1, \dots, m \quad (5)$$

where  $\Delta\phi(x,y)$  is the interference phase distribution and  $\phi_k$  is the phase-shift belonging to the  $k$ -th intensity distribution  $I_k(x,y)$ . It is important to note that  $\delta_k$  in Equation (4) is a shift in distance, while  $\phi_k$  in Equation (5) is the corresponding shift in phase.

When solving the system of equations (5) for the three unknowns  $A(x,y)$ ,  $B(x,y)$  and  $\Delta\phi(x,y)$  with the Gaussian least squares approach, the general solution for the interference phase distribution  $\Delta\phi(x,y)$  with  $m$  phase-shifts ( $m \geq 3$ ) is [11]:

$$\Delta\phi(x, y) = \arctan \frac{-\sum_{k=1}^m I_k(x, y) \sin\left(\frac{2\pi}{m}(k-1)\right)}{\sum_{k=1}^m I_k(x, y) \cos\left(\frac{2\pi}{m}(k-1)\right)} \quad (6)$$

It is important to note that this closed-form solution is based on the assumption that the phase-shift method is periodic, i.e. each phase-shift  $\phi_k$  equals  $2\pi(k-1)/m$  ( $k = 1, \dots, m$ ). This condition is satisfied because:

$$\phi_k = \frac{2\pi d}{ph} \cdot \delta_k = \frac{k-1}{m} 2\pi \quad (7)$$

The out-of-plane displacement  $z(x,y)$  is then given by:

$$z(x, y) = \frac{ph}{d} \cdot \frac{\Delta\phi(x, y)}{2\pi} \quad (8)$$

However, as mentioned above, this theory is only valid when  $z \ll h$ . When taking into account the height-dependent non-linearities, the system of equations (4) is transformed into the following system:

$$I_k = A(x, y) + B(x, y) \cdot \cos\left(\frac{2\pi d(z + \delta_k)}{p(h + z + \delta_k)}\right) \quad (9)$$

This system of equations must be solved iteratively, because the equations are non-linear in the coordinate  $z$ .

### 3. Digital phase-shift shadow Moiré method

The purpose of the digital phase-shift shadow Moiré method is to capture only one image and to perform the phase-shifts numerically. The main advantage is that dynamic measurements can be done much easier. The reference grating is placed in the illumination path only, and the camera captures the image of the projected grating lines on the deformed object surface. This digital image is saved as a bitmap pattern.

Next a virtual reference grating is created with the same pitch as the reference grating used in the experimental setup. Because the digital image was grabbed by a CCD-camera – which is in fact an observer at a finite distance from the grid – the virtual transmission function of the grid has to be corrected for the fact that both the observer and the light source are not at infinity. The expression for the virtual reference grating then is:

$$T(x) = \frac{1}{2} + \frac{1}{2} \sin \frac{2\pi}{p} \left( \frac{dz + hx}{h+z} \right) \quad (10)$$

This is precisely the second term in the Equation (2) and it must be, because the first term in Equation (2) resembles the intensity distribution of the projected grating lines, which has been captured directly by the camera.

Now the phase-shifts are introduced. Because the numerical treatment is confined to phase-shifts of the virtual reference grating in its own plane, Equation (2) must be reconsidered. Because there is only one captured image of the projected grating lines, *term 1* in Equation (2) will remain unaffected during the digital phase-shifts. Regarding *term 2*, the virtual reference grating will be given  $k$  shifts  $\delta_k$ , each equal to  $p/m$  ( $k = 1, \dots, m$ ), so that after  $k$  phase-shifts, the virtual reference grating has shifted in the  $x$ -direction over one full period. This condition establishes the relation between the shift  $\delta_k$  of the virtual reference grating and the corresponding phase-shift  $\phi_k$ :

$$\frac{2\pi}{p(h+z)} \cdot h \cdot \delta_k = \phi_k \quad k = 1, \dots, m \quad (11)$$

The contour information of each digital phase-shift is then revealed by the term:

$$(C/2) \cos \left[ \frac{2\pi(dz + h\delta_k)}{p(h+z)} \right] \quad \delta_k = \frac{k-1}{m} \cdot p \quad (12)$$

The transmission function of the virtual reference grating then becomes:

$$T_k(x) = \frac{1}{2} + \frac{1}{2} \sin \frac{2\pi(dz + h(x + \delta_k))}{p(h+z)} \quad \delta_k = \frac{k-1}{m} \cdot p \quad (13)$$

where  $T_k(x)$  is the virtual reference grating for the  $k$ -th shift ( $k = 1, \dots, m$ ).

To include the height-dependent non-linearities, the system of equations (4) must be changed into:

$$I_k = A(x, y) + B(x, y) \cdot \cos \left( \frac{2\pi(dz + h\delta_k)}{p(h+z)} \right) \quad \delta_k = \frac{k-1}{m} \cdot p \quad (14)$$

This system of equations must be solved iteratively, because the equations are non-linear in the coordinate  $z$ . The size of the shifts  $\delta_k$  ( $k = 1, \dots, m$ ) is known and remains constant, so that three unknowns have to be solved from the system of equations:  $A(x, y)$ ,  $B(x, y)$  and  $z(x, y)$ .

The last problem to solve is to find a good starting value for  $z(x, y)$  when solving the non-linear system of equations (14). Thereto the virtual reference grating  $T(x)$  must be made independent of  $z$  and is given the form:

$$T_k(x) = \frac{1}{2} + \frac{1}{2} \sin \frac{2\pi(x + \delta_k)}{p} \quad \delta_k = \frac{k-1}{m} \cdot p \quad (15)$$

where  $T_k(x)$  is the virtual reference grating for the  $k$ -th shift ( $k = 1, \dots, m$ ).

When this function is multiplied with *term 1* from Equation (2), there is no term produced which is solely dependent on  $z$ . However it concerns only a first estimate and as will be shown below, this approach works very well. So a first estimate of  $\Delta\phi(x,y)$  (and hence  $z(x,y)$ ) will be calculated from Equation (6), where the intensity distributions  $I_k$  are provided by multiplying the virtual reference grating from Equation (15) with *term 1* from Equation (2). Each shift  $\delta_k$  ( $k = 1, \dots, m$ ) is as large as the pitch divided by the number of phase-shifts ( $p/m$ ). Then the phase distribution  $\Delta\phi(x,y)$ , solved from Equation (6), must be unwrapped and the out-of-plane displacements  $z(x,y)$  are calculated from Equation (8). A first estimate for the background contrast  $A(x,y)$  and the local contrast  $B(x,y)$  can be calculated from the expressions:

$$A = \frac{\sum_{k=1}^5 I_k}{5} \tag{16}$$

$$B = \left(\frac{2}{5}\right) \sqrt{\left[\sum_{k=1}^5 I_k \cos\left(\frac{k-1}{5} 2\pi\right)\right]^2 + \left[\sum_{k=1}^5 I_k \sin\left(\frac{k-1}{5} 2\pi\right)\right]^2}$$

With these estimates for  $A(x,y)$ ,  $B(x,y)$  and  $z(x,y)$ , the system of equations (14) can be solved iteratively.

It is important to note that this digital simulation to find a starting value for  $z(x,y)$  fundamentally differs from a linear solution of the mechanical phase-shifting procedure. Indeed, the influence of  $z$  on the virtual reference grating (Equation (15)) is completely neglected, while this  $z$ -information of the grating is present in each of the recorded intensity distributions with the mechanical phase-shifts in the  $z$ -direction, even if the height-dependent non-linearities are not included.

#### 4. Verification of the proposed theory

The theory is applied to an experiment, in which the out-of-plane displacements  $z$  are not negligible compared to the distance  $h$  ( $h_1 = h_2$ ) from the reference grating to the observer and the light source. The object surface is a rectangular plate, which is clamped at the upper side and which is bent at the lower side. The maximum out-of-plane displacements  $z$  are between 10 and 20 millimeters and the distance  $h$  is approximately 300 millimeters. Figure 2 shows the experimental setup.

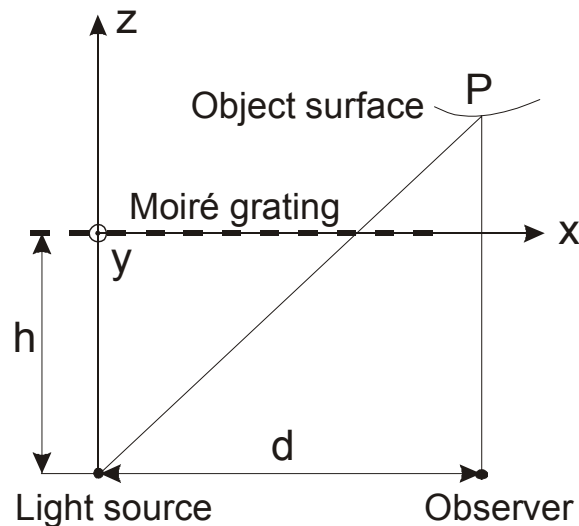


**Figure 2** Experimental setup with the reference grating placed only in the illumination path.

The light source is a non-collimated pointlike white-light source. The CCD-camera has a resolution of 2.5 Megapixels. Because the corresponding size of one pixel must be known, a picture is captured, where the reference grating is photographed as well. From the well-known pitch of the grating and the corresponding number of pixels, the pixel size can be determined. Figure 3 shows the digital image. The left side shows the reference grating with the fringe pattern yielded by standard shadow Moiré. The right side shows the shadow of the grating lines onto the bent object surface.

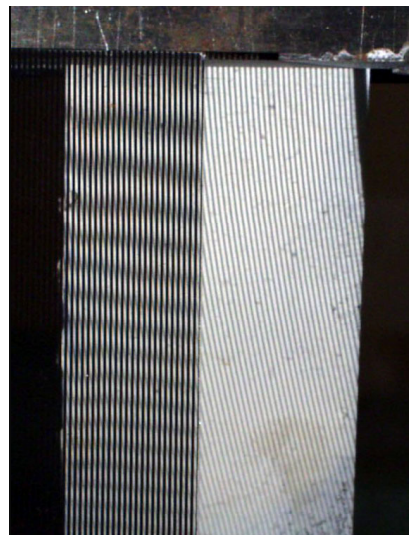


**Figure 3** Captured image with the Moiré contouring (left) and the shadow of the reference grating (right).

First of all the proposed theory has been validated against the standard phase-shift shadow Moiré technique, where at least three (and better five) images of the respective phase-shifts are recorded separately with mechanical phase-stepping devices.

Thereto a standard phase-shift shadow Moiré setup (Figure 1) has been used and the grid is shifted five times in the  $z$ -direction. While recording the fringe pattern, the grid is translated in

its own plane to remove the individual grating lines of the reference grating, according to the technique described by Allen and Meadows [12] and Dirckx et al. [13]. The grid is moved continuously in its plane during exposure. As a consequence the transmission function of the grid is also a function of time. When the expression for the transmission function is expanded into a Fourier series, it can be seen that all the noise terms are averaged out since the average of a sine wave over a period is zero.

Now a comparison is made between four calculations of the out-of-plane profile with different assumptions:

Mechanical phase-stepping:

- 1) the first estimate for  $z$  is derived from the system of equations (4). This is a simplified solution, because it is assumed that  $z \ll h$ .
- 2) the non-linear solution of the system of equations (9) yields a second out-of-plane displacement profile for the object surface, which can be considered as the most accurate one.

Digital phase-stepping:

- 3) the guess value for  $z$  is derived from the system of equations (5) with the virtual reference grating  $T(x)$  from Equation (15). This is in fact the most simplified solution, because there is no  $z$ -dependence in the expression for the virtual reference grating.
- 4) the general solution of the system of equations (14) yields a last out-of-plane displacement profile for the object surface.

Figure 4 shows the out-of-plane displacement profiles.

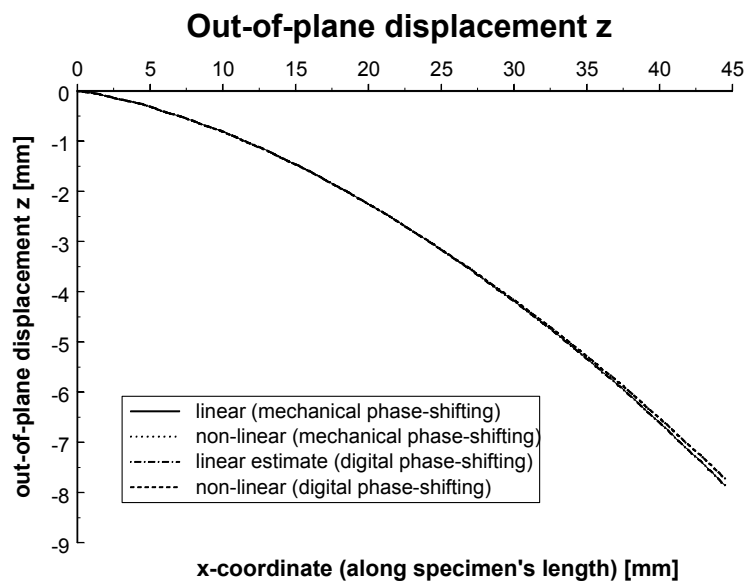
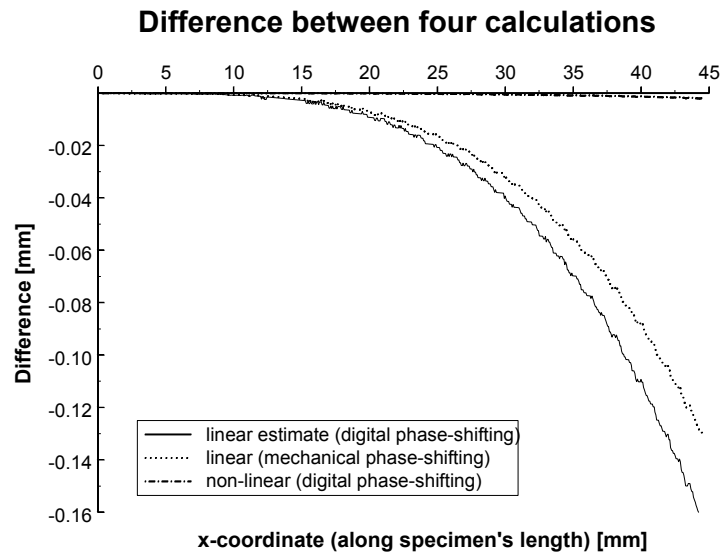


Figure 4 Out-of-plane displacement  $z$  for the different calculations.

It can be seen from Figure 5 that the predictions of the different calculations are very close for small  $z$ -displacements, but differ significantly for larger  $z$ -displacements.



**Figure 5** Difference between the out-of-plane displacements of the four calculations.

In this Figure the non-linear solution with mechanical phase-shifting has been taken as the reference profile and coincides with the abscissa. The non-linear digital phase-shifting solution is almost identical to the mechanical one, but the linear solution with mechanical phase-shifting leads to considerable differences for large z-displacements (0.13 mm with the non-linear mechanical phase-shifting solution for  $x = 45$  mm). This clearly demonstrates that one must take into account height-dependent non-linearities when measuring micro deformations of curved surfaces. It is also demonstrated that the starting value for the non-linear digital phase-stepping solution is naturally the worst case solution, but appears to be a good guess value to start the iterative solution of the system of equations (14).

## 5. Application to micro fatigue damage measurement

The proposed technique has shown to be very useful to quantify micro fatigue damage in fibre-reinforced composite materials. In Figure 6, the bending shape of a rectangular composite specimen is shown, where the upper side of the specimen is clamped and the lower side is given a certain bending displacement. During fatigue life, damage is growing steadily and the out-of-plane displacement profile is severely changing.

The small ripples in the curves correspond to very small inequalities of the specimen surface, which are due to the coat of paint on the surface.

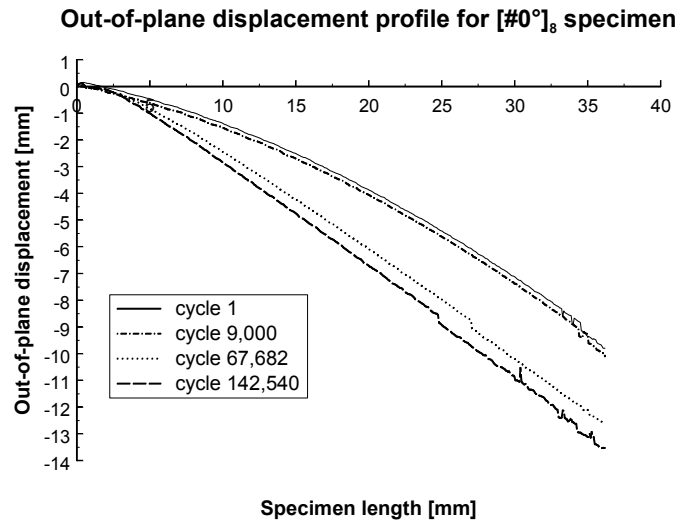


**Figure 6** Out-of-plane displacement profile for a composite specimen.

The standard phase-shift shadow Moiré method has serious disadvantages in this case. At least three and better five phase-shifts are required to solve for the unknown background contrast  $A(x,y)$ , local contrast  $B(x,y)$  and interference phase distribution  $\Delta\phi(x,y)$ . Hence, every time that the fatigue test is stopped to record the out-of-plane displacement profile, five phase-shifts should be performed. Since the measurement procedure should be automated (to keep the fatigue tests running day and night), an accurate set of computer-controlled phase-stepping devices would be required.

With the digital phase-shift shadow Moiré method proposed here, the reference grating is placed in the illumination path only, and the digital camera captures the image of the shadow projection onto the deformed object surface of the reference grating lines “on the run”. Further, due to the simple optical arrangement, the errors caused by optical settings are eliminated. The distances of the curved surface to the reference grating are large and when one wants to measure micro deformations of this surface, the initial state has to be calculated with the non-linear iterative approach.

The measured out-of-plane profiles are then correlated through finite element calculations with the damage distribution in the cross-sections, because the bending stiffness of each cross-section is directly related with the out-of-plane displacement profile.

Figure 7 shows a micrograph of the fatigue damage at the clamped end of the specimen.

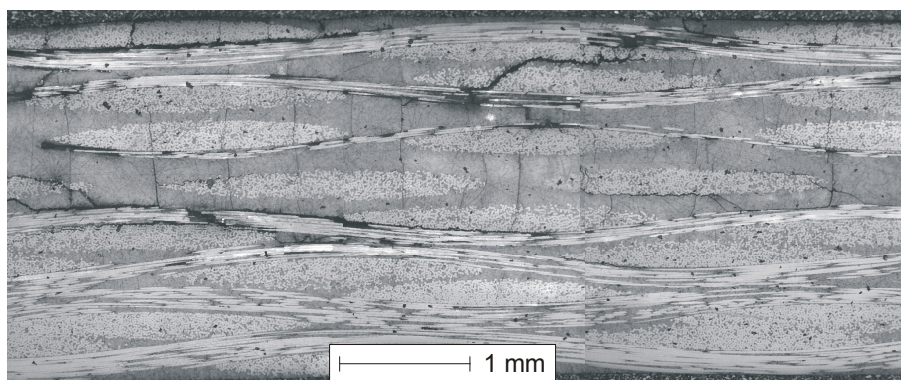


**Figure 7** Micrograph of the fatigue damage at the clamped end of the composite specimen.

The microscopic failure mechanisms (matrix cracking, fibre fracture and meta-delaminations) at the tensile side correspond very well with the hinge observed in the recorded displacement profile.

## 6. Conclusions

A digital phase-shift shadow Moiré technique was proposed, where only one image has to be taken: the projection of the reference grating lines onto the deformed object surface. The virtual reference grating is superimposed numerically. Moreover the phase-shifts are calculated by shifting the virtual reference grating in its own plane, taking into account that the observer and the light source are at a finite distance from the grid.

Often it is assumed that the influence of the  $z$ -distance between the curved surface and the reference grating is negligible compared to the distances between light source, camera and reference grating. In this case the assumption is not valid and the system of equations resulting from the phase-shift algorithm is solved iteratively. It appears that the general non-linear solution differs considerably from the simplified linear solution for larger  $z$  distances.

Due to the fact that only one image is captured, the errors caused by miscalibration and misalignment of phase-stepping devices are eliminated.

It is worthwhile to note that the numerical phase shifting procedure could also be performed in the spatial or frequency domain, since the projected lines themselves contain the phase information. However the non-linear relationship between the  $z$  distance and the phase remains, and the advantage of the presently formulated equations is that they include all information about the experimental setup (distances between light source, digital camera and reference grating). So no calibration is needed when the experimental layout has been changed.

## Acknowledgements

The author W. Van Paepegem gratefully acknowledges financial support through a grant of the Fund for Scientific Research – Flanders (F.W.O.).

## References

1. Yi-Bae, C. and Seung-Woo, K. (1998). Phase-shifting grating projection moiré topography. *Optical Engineering*, 37(3), 1005-1010.
2. Peng, X., Gao, Z. and Zhou, S.M. (1995). Surface contouring by a new type of digital moiré technique. *Optik*, 100(2), 63-67.
3. Peng, X., Zhu, S.M., Su, C.J. and Tseng, M.M. (1999). Model-based digital moiré topography. *Optik*, 110(4), 184-190.
4. Dirckx, J.J., Decraemer, W.F. and Dielis, G. (1988). Phase shift method based on object translation for full field automatic 3-D surface reconstruction from moire topograms. *Applied Optics*, 27(6), 1164-1169.
5. Yoshizawa, T. and Tomisawa, T. (1993). Shadow moiré topography by means of the phase-shift method. *Optical Engineering*, 32(7), 1668-1674.

6. Henao, R., Tagliaferri, A. and Torroba, R. (1999). A contouring approach using single grating digital shadow moiré with a phase stepping technique. *Optik*, 110(4), 199-201.
7. Meadows, D.M., Johnson, W.O. and Allen, J.B. (1970). Generation of surface contours by moiré patterns. *Applied Optics*, 9(4), 942-947.
8. Takasaki, H. (1970). Moiré topography. *Applied Optics*, 9(6), 1467-1472.
9. Takasaki, H. (1973). Moiré topography. *Applied Optics*, 12(4), 845-850.
10. Kujawinska, M. and Osten, W. (1998). Fringe pattern analysis methods: up-to-date review. *Proceedings SPIE*, 3407, 56-66.
11. Kreis, T. (1996). *Holographic interferometry - Principles and methods*. Chapter 4: Quantitative evaluation of the interference phase. Berlin, Akademie Verlag, pp. 101-170.
12. Allen, J.B. and Meadows, D.M. (1971). Removal of unwanted patterns from moiré contour maps by grid translation techniques. *Applied Optics*, 10(1), 210-212.
13. Dirckx, J.J., Decraemer, W.F. and Eyckmans, M.M. (1990). Grating noise removal in moiré topography. *Optik*, 86(3), 107-110.